

# Interplanetary magnetic field power spectra with frequencies from $2.4 \times 10^{-5}$ Hz to 470 Hz from HELIOS-observations during solar minimum conditions

K.U. Denskat<sup>1</sup>, H.J. Beinroth<sup>1</sup>, and F.M. Neubauer<sup>2</sup>

<sup>1</sup> Institut für Geophysik und Meteorologie der Technischen Universität Braunschweig, Mendelssohnstr. 3, D-3300 Braunschweig, FRG

<sup>2</sup> Institut für Geophysik und Meteorologie der Universität zu Köln, Albertus-Magnus-Platz, D-5000 Köln 41, FRG

**Abstract.** By using data from the Technical University of Braunschweig flux-gate and search-coil magnetometer experiments on board of Helios 2 we study the spectral properties of the interplanetary magnetic field over a frequency range from  $2.4 \times 10^{-5}$  Hz up to 470 Hz. Examples of power spectral density estimates at different heliocentric distances are shown as well as the change of the spectra during the progress of a high speed stream. A general feature of the spectra is that in a log-log spectral representation the steepness of the power spectral density estimates varies as a function of frequency. If we relate the spectral densities by a power law  $P \sim f^{-\alpha}$ , the spectral index  $\alpha$  increases with increasing frequency. At 1 AU  $\alpha$  varies on average from 1.6 to 3.4 and at 0.3 AU from 1.0 to 3.4, the major changes in the spectral index occurring at low frequencies. In addition, just within the frequency gap between the two experiments, between 2 Hz and 4.7 Hz, an inflexion point is inferred from the spectrum above and below this frequency range. This spectral feature can at least partly be attributed to the damping of the Alfvén-mode waves near the proton and also  $\alpha$ -particle cyclotron frequencies.

The observed power spectra are compared with models of MHD turbulence and it is found that at least some of the properties of MHD turbulence fit the observations remarkably well.

**Key words:** Interplanetary magnetic field – Solar wind plasma – Hydromagnetic waves and turbulence

## Introduction

The past one and a half decades brought an increasing number of observational and theoretical studies on waves, discontinuities and instabilities in the solar wind plasma. Most reported observations of magnetic fluctuations in the interplanetary plasma show fluctuations with frequencies well below the local proton gyrofrequency. A comprehensive review on theory and observations of MHD-fluctuations is available from Barnes (1979). Only recent instruments on the HELIOS and to some extent the VOYAGER spacecraft have background noise levels low enough to monitor the magnetic component of the fluctuations in the frequency regime between the local proton and electron

gyrofrequency at distances from the sun other than 1 AU (Neubauer et al. 1977a, b; Behannon, 1978). Up to now the interpretation of observed magnetic fluctuations was done separately for those fluctuations well above or well below the proton gyrofrequency. An exception is the work of Behannon (1976), who reported interplanetary magnetic field power spectra from  $10^{-4}$  to 12.5 Hz obtained during the Mariner 10 mission. With the HELIOS flux-gate and search-coil magnetometer we are able to monitor the interplanetary magnetic field from dc-conditions up to the local electron gyrofrequency. In this work we will present the spectral properties of magnetic fluctuations in the solar wind plasma from  $2.4 \times 10^{-5}$  Hz up to 470 Hz (at 0.3 AU). The lower frequency limit was selected to exclude major influences of different solar wind stream conditions on the power spectral density estimates. The high frequency limit is given by the observed magnetic wave activity exceeding the instrument noise levels. This frequency limit varies between 47 to 100 Hz at 1 AU and 470 Hz at 0.3 AU for power spectral density estimates averaged over several hours. On a finer time scale, magnetic wave activity is also observed at higher frequencies.

The plan of the paper is the following: First we describe briefly the instrumentation, measuring method and raw data analysis as far as is necessary to understand the results. In the following section, after presenting a short summary of the algorithm used for the computation of the power spectral density estimates from the flux-gate magnetometer data, we give examples of magnetic field power spectra observed at different heliocentric distances as well as the variation of the spectra in the course of a high speed stream. In the following section we discuss the observations and try an interpretation of the observed power spectra in terms of waves as well as in terms of MHD-turbulence. In the last section we briefly summarize the results.

## Instrumentation and data analysis

On board each of the two spin-stabilized HELIOS spacecraft, the Institute for Geophysics and Meteorology of the Technical University of Braunschweig provided two magnetometers, a three component flux-gate magnetometer (Förster-sonde) for observing, in real time, the interplanetary magnetic field up to 2 Hz and a

three-component search-coil magnetometer designed to observe the high frequency component of magnetic fluctuations in the interplanetary medium in the frequency range from 4.7 Hz to 2.2 kHz. This instrumentation enables us to study the large scale properties of the interplanetary magnetic field as well as the magnetic component of different wave modes with frequencies from well below the local proton gyrofrequency up to the local electron gyrofrequency. Since detailed descriptions of the experiments have been given elsewhere (flux-gate magnetometer: Musmann et al., 1975; search-coil magnetometer: Dehmel et al., 1975), here we shall present only a short summary of the experiments, their measuring method and their data analysis necessary to understand the results presented in the following sections.

### Flux-gate magnetometer experiment

The flux-gate magnetometer has two automatically switchable measurement ranges of up  $\pm 400$  nT with a highest resolution of  $\pm 0.2$  nT and a maximum sampling rate of 8 vectors/s. The data used throughout this paper were obtained within the measurement ranges of  $\pm 100$  nT with the highest resolution of  $\pm 0.2$  nT and a sampling rate of 4 vectors/s. A mechanical flipper device is included in the instrument which makes it possible to flip by command the sensor parallel to the spin axis into the spinning plane of the spacecraft to help determine the zero-offset of the Z-component parallel to the spin axis. In addition the offset of the Z-component is determined continuously by a correlation technique (Hedgecock, 1975a). The overall offset of the components in the spin plane composed of sensor offsets and spacecraft field are removed by properly averaging over the spin variation taking into account the misalignment between the geometric and magnetic axes of the instrument, where the misalignment angles are calculated from the data (e.g. Neubauer et al., 1981). An aliasing filter is included which helps keep the contribution of power above the Nyquist frequency to power below this frequency to a minimum.

In this study we use detailed data of the interplanetary vector magnetic field with samples every 0.25 s as well as 40 s averages. The coordinate system used is the solar-ecliptic (SE) coordinate system, where X is taken along the observer-sun line and is directed to the sun, Z is directed to the north-ecliptic pole and Y completes the right-handed orthogonal set.

### Search-coil magnetometer experiment

The sensor unit of the search-coil magnetometer experiment consists of three orthogonally oriented search-coil sensors mounted with the Z-sensor parallel to the spin-axis and the X- and Y-sensor in the spin plane. The output voltage of each sensor-preamplifier is proportional to the time derivative of the component under consideration. Further processing is done by a spectrum analyzer consisting of two sets of eight bandpass filters spaced logarithmically in frequency, where one is used for the Z-component, the other one for the X- or Y-component. A digital mean-value-computer squares and averages the filter outputs over successive time

intervals of lengths  $T_A$ , where all filters are processed in parallel. For the data used in this study  $T_A$  was 1.125 s. The mean square values  $M_n$  are related to the power spectral density  $P(f)$  of a given component of the magnetic field by (Neubauer et al., 1977a)

$$M_n = \int_0^{\infty} |T_n(f)|^2 f^2 P(f) df \quad (1)$$

where  $T_n(f)$  is the complex transfer function of filter  $n$  which quickly tends to 0 beyond the 3 dB-points of each filter. The power spectral densities  $\bar{P}_n$  assigned to the center frequencies  $f_{cn}$  of each filter are given by

$$\bar{P}_n = \frac{M_n}{\Delta f_n f_{cn}^2} = \int_0^{\infty} |T_n(f)|^2 \left(\frac{f}{f_{cn}}\right)^2 P(f) \frac{df}{\Delta f_n}$$

or

$$\bar{P}(f_{cn}) \approx \int_{f_{in}}^{f_{un}} P(f) \left(\frac{f}{f_{cn}}\right)^2 \frac{df}{\Delta f_n} \quad (2)$$

Here  $f_{in}$  and  $f_{un}$  are the lower and upper frequency limits of filter  $n$ , and  $f_n = f_{un} - f_{in}$  is the bandwidth. For further analysis 40 s averages of power spectral densities have been used.

We emphasize that the use of the digital mean-value-computer guarantees an accuracy for the power spectral density estimates not achieved by interplanetary wave experiments in the past. Only this high accuracy allows the presentation (and interpretation) of high-frequency power spectral density estimates from a search coil experiment together with low-frequency power spectral density estimates from flux-gate-magnetometer data.

### Power spectral density estimates of the interplanetary vector magnetic field

The method used for computing power spectral density estimates from a digital time series is presented below. For the power spectral density estimates from the search coil instrument no further calculations are necessary except proper averaging over the time interval needed.

#### Power spectral analysis from digital time series

For the computation of power spectra we generally follow the procedure described by Bendat and Piersol (1971, p. 322ff). Since we are using the fast Fourier transform technique the data intervals were chosen such that the number of data fits a power of 2. By taking 1024 data points for each Fourier transform the 40 s magnetic field averages limit the largest wave period which can be analyzed to 11 h and 23 min. By taking detailed data (one vector every 0.25 s) one Fourier transform is computed over a time period of 256 s. In order to get a composite power spectrum from  $2.4 \times 10^{-5}$  Hz up to 2 Hz we must compute 170 spectra from the detailed data (each time overlaps the foreground by 16 s) and average the resulting power spectral density estimates for each frequency.

Low order trends were removed by subtracting the values predicted by a "least squares" fitted second or-

der polynomial. After the data were reduced to zero mean and data gaps were filled by zeros the data sequences were tapered by a cosine taper data window. Then the Fourier transform was performed and the raw spectral estimates were computed. The raw spectral estimates were frequency averaged to obtain an equivalent degree of freedom of 32. For the spectra from detailed data the additional segment averaging leads to an equivalent degree of freedom of 5440. We limited our analysis to data sequences having data gaps less than 5%. We further excluded a data sequence from the analysis if the data breaks appeared regular in occurrence. Since missing data are filled by zeros (zero being the most probable value in the Gaussian amplitude distribution of prepared data) jumps at the beginning and the end of data gaps may cause power enhancements which are quite difficult to estimate. A contribution to the total power spectral density owing to data gaps may be computed from applying Parseval's Theorem (e.g. Jenkins and Watts, 1968, p. 215). Hedgecock (1975b) also used this procedure to check and correct the amplitudes of magnetic field power spectral densities. A power spectral density estimate was only accepted if Parseval's Theorem

$$\sigma^2 = \int_{f_1}^{f_2} P(f) df \quad (3)$$

was fulfilled. Here  $\sigma^2$  is the variance of a field component,  $P(f)$  the power spectral density estimate, and  $f_1$  and  $f_2$  are the frequency limits of the spectrum.

The possible noise sources do not cause any problems in our analysis. Quantization and instrument noise are both below  $10^{-2} \text{ nT}^2/\text{Hz}$  at the highest frequency inherent in the analysis. The results shown in the next section reveal that the power spectral densities are always above the noise level. This is in general true for all time periods where the spacecraft were close to the sun. Only under very quiet conditions in the interplanetary medium near 1 AU does the power spectral density reach the noise level at high frequencies.

#### Observations at 0.3 AU and 0.98 AU

In Figs. 1 and 2 we present representative power spectral density estimates of the Z-component of the interplanetary vector magnetic field at 0.30 AU and at 0.98 AU. Up to 2 Hz the spectral densities are computed from the fluxgate magnetometer data, from 4.7 Hz to higher frequencies the spectral densities were measured by the search-coil magnetometer experiment. The frequency range of spectral densities is limited at high frequencies by the instrument noise level and at low frequencies by the choice of the longest period inherent in the analysis. Spectral studies in the MHD regime (frequency range up to  $1.2 \times 10^{-2}$  Hz) are already contained in Denskat and Neubauer (1982). Presenting only one component does not mean a lack of generality, since the general features of the spectra for the components in the ecliptic are very much the same, although the magnitude may be slightly different.

The two examples at different heliocentric distances were chosen within time periods under similar solar wind conditions where the solar wind speed was high

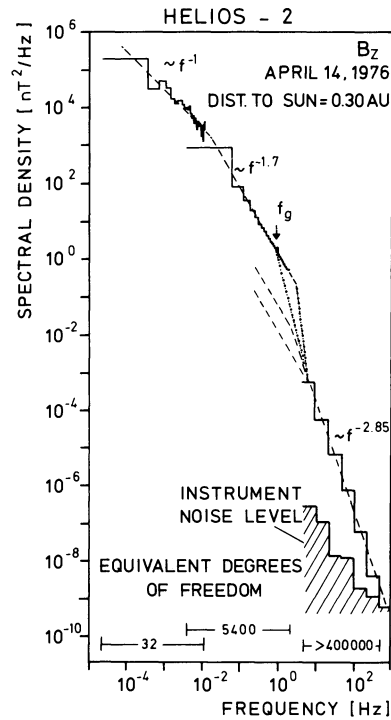


**Fig. 1.** Power spectral density estimates of the magnetic vector field component  $B_z$  from the HELIOS-2 fluxgate and search coil magnetometer experiment at a heliocentric distance of 0.30 AU. In the frequency range from  $2.4 \times 10^{-5}$  Hz to  $1.3 \times 10^{-2}$  Hz the spectral density was computed from 40s averages of fluxgate magnetic field data. In the range from  $3.9 \times 10^{-3}$  to 2 Hz the spectral densities were computed from detailed fluxgate samples every 0.25s. The spectral densities above 4.7 Hz were measured by the search coil magnetometer experiment. The dashed lines give power law fits (determined by a least mean square method) assuming  $P \sim f^{-\alpha}$  for the different frequency regimes. The dashed and dotted lines are explained in the text. The statistical confidence limits of the spectral density estimates are given by the equivalent degrees of freedom (DF). E.g. for 32 DF 95% confidence limits are  $[0.65 P(f), 1.75 P(f)]$ , for 5400 DF these limits are  $[0.99 P(f), 1.01 P(f)]$ . At high frequencies the spectrum is limited by the signal becoming smaller than the instrument noise level of the search coil magnetometer experiment. The flux-gate magnetometer noise is always smaller than  $10^{-2} \text{ nT}^2/\text{Hz}$ .

with no influence of the leading edges of the two streams. Despite the similar solar wind conditions the spectra are quite different especially in certain frequency bands which will be discussed and interpreted in the next chapter.

The evolution of power spectra in the course of high speed streams is another interesting subject. In Fig. 3 power spectral density estimates of  $B_z$  are shown as a function of time and stream structure. The first spectra are obtained during quiet interplanetary conditions at a heliocentric distance of 0.34 AU (Marsch et al., 1982a). On 11 April 1976 the plasma starts being compressed with a proton density increase from  $60 \text{ cm}^{-3}$  to  $185 \text{ cm}^{-3}$  within two days. Behind the region of compressed plasma the proton velocity increases from about  $350 \text{ km s}^{-1}$  up to  $760 \text{ km s}^{-1}$  in the center of the high speed stream. The magnetic field

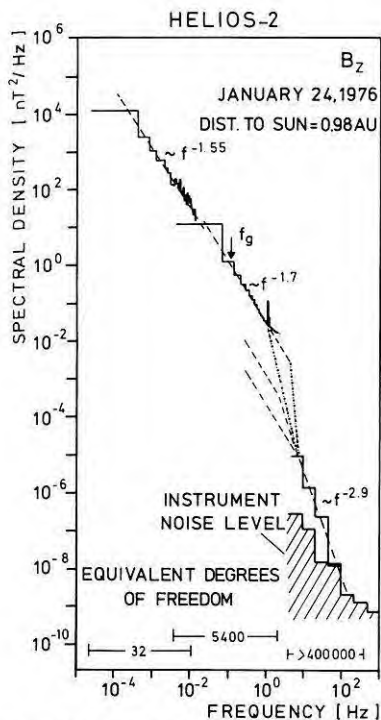


Fig. 2. Same as Fig. 1 obtained at a heliocentric distance of 0.98 AU

strength varies between 28 nT and 44 nT. Apparently the power spectral density estimates are different at different locations of the high speed stream and different as well from those spectral density estimates in the low speed plasma before the onset of the high speed stream. These differences are most pronounced at low frequencies up to  $10^{-3}$  Hz and at high frequencies above 4.7 Hz.

In the region of the compressed plasma the spectral density estimates of  $B_z$  are enhanced at low frequencies indicating local wave generation. In addition the spectra in this frequency range are much steeper than in the center of the high speed stream. The frequency range from  $4 \times 10^{-3}$  Hz to 2 Hz shows enhanced spectral density estimates together with the onset of increasing solar wind speed. At high frequencies above 4.7 Hz the most obvious feature is the drastic spectral density enhancement between 4.7 Hz and above 100 Hz in the compression region indicating local wave generation and between 4.7 Hz and 470 Hz in the region of increasing solar wind speed in contrast to the most regular occurrence of the spectra in the center of the high speed stream.

### Interpretation and discussion

The power spectral density estimates obtained from observations at different locations in the interplanetary medium (Figs 1 and 2) clearly show that the heliocentric distance plays an important role for the evolution of the interplanetary magnetic field fluctuations. At all frequencies the power spectral density is decreasing with increasing heliocentric radius together with a gen-

eral decrease of the magnetic field strength from about 44 nT at 0.29 AU to 6 nT at 1.0 AU. The slope of the spectra does not change significantly from  $4 \times 10^{-3}$  Hz to  $10^2$  Hz. The statistical properties of the spectral density as a function of distance in the frequency range of the search-coil magnetometer experiment are given in detail by Beinroth and Neubauer (1981). However, the slope of the spectral density in the frequency range below  $4 \times 10^{-3}$  Hz changes drastically. Magnetic fluctuations in the MHD regime observed by HELIOS 1 and 2 have been studied by Denskat and Neubauer (1982) (frequency range from  $2.4 \times 10^{-5}$  to  $1.2 \times 10^{-2}$  Hz) and by Bavassano et al. (1982) (frequency range from  $2.8 \times 10^{-4}$  to  $8.3 \times 10^{-2}$  Hz). The authors of both studies found a variation of the spectral index with varying heliocentric distance, where the spectra become increasingly steeper with increasing heliocentric distance at frequencies below  $4 \times 10^{-3}$  Hz. Denskat and Neubauer come to the conclusion that the solar wind acts as a low pass filter for MHD-waves (the magnetic component of which is observed in this frequency range well below the proton gyrofrequency) meaning that MHD waves with periods less than about 15 minutes (in the measuring system) are damped on their way out from the sun from 0.3 to 0.98 AU. Furthermore Denskat and Neubauer have shown that most of this damping occurs within a heliocentric distance of approximately 0.4 AU. The general tendency of the directional fluctuations of the interplanetary vector magnetic field is that the slope of the power spectral densities as a function of frequency becomes steeper with increasing frequency. This is true for all heliocentric distances but stronger for distances within 0.4 AU, where the spectral slope changes from being proportional to  $f^{-1}$  to  $f^{-3}$  as a function of frequency.

Both power spectra shown have a peak in spectral density at 1 Hz, where the larger effect occurs in the case of the spectrum at 0.98 AU. This effect is due to the difficulty of totally removing the 1 Hz spacecraft spin period. The effect is only small at 0.3 AU, where the magnetic field is high ( $\sim 42$  nT). Due to the minor effect of the digitization window the misalignment angles and zero offsets of the magnetometer experiment could be computed quite accurately. At low magnetic field intensities of  $\sim 6$  nT at 0.98 AU the effect of the digitization window is larger finally leading to enhanced spectral density estimates at 1 Hz and - by leakage - at the surrounding frequencies. Therefore in the case of the spectrum at 0.98 AU the frequency range from 0.8 to 2 Hz should be considered with caution. On the other hand the only tiny enhancement in spectral density at 1 Hz in the case of the spectrum at 0.3 AU makes us confident that at least under high magnetic field conditions the effects mentioned above do not essentially influence the spectrum in any frequency range.

The power spectra shown clearly reveal an unfortunate property of the frequency coverage of the experiments: The major changes in the slope of the spectral density as well as a displacement between parts of the spectra occur within the frequency band from 2 to 4.7 Hz not covered by the two experiments. Therefore we must discuss in some detail why these drastic changes occur. We start with a discussion in terms of

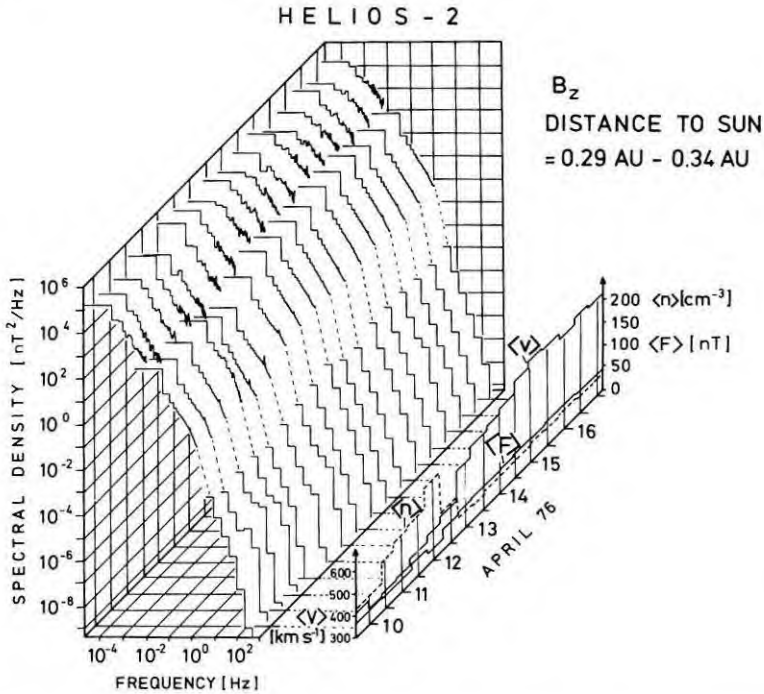


**Fig. 3.** Sequence of interplanetary magnetic field power spectral density estimates over a high speed solar wind stream at the first perihelion passage of HELIOS-2 in April 1976. The small box on the right gives 11-hour averages of solar wind proton bulk speed, proton density, and magnetic field strength

electro-magnetic wave fields followed by a complementary discussion in terms of MHD-turbulence.

#### *Superposed wave modes*

At the beginning of this discussion we have to carefully review the various wave modes possible in a hot magnetized plasma. The linear theory of wave propagation in a hot collisionless magnetoplasma described by the Vlasov-Maxwell set of equations (e.g. Montgomery and Tidman, 1964) yields an infinite number of wave modes most of which are strongly damped. At very low frequencies below the dominant ion cyclotron frequency there are three important wave modes: the Alfvén wave and the fast and slow magnetoacoustic waves (e.g. Barnes, 1979). At oblique angles of propagation the three wave modes are clearly distinct by their propagation velocities and the characteristics of the wave perturbation quantities. They are linearly polarized in the magnetic field and velocity vector perturbations. As the case of propagation parallel to the magnetic field is approached one of the magnetoacoustic modes becomes indistinguishable from the Alfvén waves. In the case of the Alfvén speed  $V_A$  being greater than the sound speed  $V_s$  it is the fast magnetoacoustic mode which degenerates into an Alfvén wave at  $\theta=0$ , where  $\theta$  is the angle between the propagation vector  $\mathbf{k}$  and the background magnetic field. For  $V_A < V_s$  the slow mode degenerates into an Alfvén wave at  $\theta=0$ . The alternate magnetoacoustic mode for  $\theta=0$  in each case is the sound wave the collisionless counterpart of which is the ion acoustic wave which has been observed by Gurnett and Frank (1978) and Kurth et al. (1979 a, b) in the solar wind. At oblique angles  $\theta$  it also develops magnetic components including magnitude variations. It is clear from this brief discussion of the possible wave modes at low frequencies i.e. in the MHD-range that the usual identification of Alfvén waves in the solar

wind using the relationship between the fluctuations in vectorial velocity and magnetic field and the lack of density and magnitude variations has some arbitrariness. The Alfvén waves may be contaminated by some magnetoacoustic wave energy at small  $\theta$ . A satisfactory solution of this problem could be achieved by resolving the  $\mathbf{k}$ -vector distribution of waves in the solar wind with an array of satellites. The part of the wave energy which is being accounted as Alfvén wave energy but really belongs to a magnetoacoustic mode could then be obtained from the continuity of wave energy as a function of  $\theta$  for every mode. Since the degeneracy of wave modes is serious at small  $\theta$  only the observations by Denskat and Burlaga (1977) are significant in that they show that the solar wind fluctuations cannot be described by plane wave fields with  $\mathbf{k}$  parallel to the magnetic field but rather a broad distribution of  $\mathbf{k}$ -vectors around the average  $\mathbf{B}$ -vector. Hence the fluctuations well below the proton gyro frequency can be thought to consist mainly of Alfvénic waves (Denskat et al., 1981). However, fluctuations in magnetic field strength and plasma density indicate the additional presence of magnetoacoustic wave modes and/or static structures (Burlaga and Turner, 1976; Denskat and Burlaga, 1977). The contribution of magnetoacoustic wave modes to the overall power level in the solar wind plasma was estimated to be up to a quarter (Sari and Valley, 1976). Whether or not the contribution of magneto-acoustic wave modes to the total power level is that high, there is general agreement in the literature that the major part of the fluctuations in the MHD-region well below the proton gyrofrequency consists of Alfvénic waves with an admixture of magnetoacoustic waves and static structures (i.e. tangential discontinuities).

The degeneracy between two of the MHD-wave modes at  $\theta=0$  disappears for  $\theta \neq 0$ . It also disappears for finite frequencies. At a finite frequency well below

the applicable ion gyro frequency a range of angles  $\theta$  from zero to  $\theta_c$  exists in which the wave modes start to be circularly polarized at  $\theta=0$  and become progressively linearly polarized above  $\theta_c$ . Here  $\theta_c$  increases with frequency. In this more accurate description the Alfvén wave proper is polarized in the left hand i.e. ionic gyration sense. Since left hand polarization has not been observed in the solar wind at low frequencies we conclude in agreement with the discussion above that the range of  $\mathbf{k}$ -vectors generally exceeds  $\theta=\theta_c$  by an appreciable amount. As the frequency approaches the  $\text{He}^{++}$  and proton cyclotron frequencies the Alfvén waves are damped severely by ion cyclotron damping. Hence we expect an appreciable drop in power spectral density which is somewhat stretched out in frequency due to the Doppler shifts. The remaining power spectral densities at high frequencies then represent the continuation of the  $R$ -mode which at very low frequencies is a magnetoacoustic wave mode into the “whistler mode” range above the proton gyro frequency. We therefore attribute the drop in spectral density between  $\lesssim 2\text{ Hz}$  and  $4.7\text{ Hz}$  to the damping of the Alfvén wave portion of the wave spectrum which, close to the ion gyro frequencies, are generally referred to as ion cyclotron waves. In the plasma rest frame the damping occurs near the proton cyclotron frequency at a frequency  $f$  which is Doppler shifted to  $f'$  in the frame of HELIOS with

$$f' = f(1 + V_s/V_p \cdot \cos\beta) \quad (4)$$

where  $V_p$  is the phase velocity and  $\beta$  the angle between the solar wind vector and the  $\mathbf{k}$ -vector under consideration.  $f'/f$  is a complex function of frequency, direction of propagation and magnetoplasma parameters (e.g. Denskat, 1975). For example, outwardly propagating Alfvén waves have a maximum Doppler ratio (as a function of  $\theta$ ) of  $f'/f=8$  at  $0.98\text{ AU}$  and  $5$  at  $0.3\text{ AU}$  for typical conditions. For the same distances the proton gyro frequencies are  $0.09\text{ Hz}$  and  $0.7\text{ Hz}$ , respectively. Since the Doppler ratio  $f'/f$  grows with increasing distance the frequency at which the most pronounced drop occurs varies more slowly than the proton gyro frequency. Taking into account the somewhat reduced confidence in the spectral densities around  $1\text{ Hz}$  we may conclude that the observations are at least qualitatively in agreement with the ideas developed above. Possible variations of the total spectral densities across the gap are indicated by dotted lines. The possible contribution of the magneto-acoustic component is indicated by dashed lines.

### Turbulence

Until now we interpreted the solar wind magnetic field fluctuations in terms of waves. An alternate but not mutually exclusive view is to consider the solar wind as a turbulent medium. By using Kraichnan's (1965) incompressible MHD turbulence theory Coleman (1968) interpreted power spectra of the magnetic field and the radial component of the solar wind velocity in terms of turbulence. Coleman assumed the energy to be available because of the differential flow in the solar wind. Through the operation of some undetermined insta-

bility this energy should be fed into the energy-range spectrum of the turbulence,  $10^{-5}\text{ Hz} < f < 10^{-4}\text{ Hz}$ , and the differential motion is dissipated. The energy then cascades through the inertial-range spectrum of the turbulence,  $10^{-4}\text{ Hz} < f < 10^{-1}\text{ Hz}$ , where the turbulence in the inertial range should be composed of a hierarchy of Alfvén waves. Livshits and Tsytovich (1970) developed a theory of hydromagnetic turbulence spectra in collisionless plasma and concluded that a power law fluctuation spectrum is stable for a spectral exponent  $\alpha \geq 1$ , at least when the Alfvén speed is large in comparison with the electron and ion thermal speeds. The same conclusion for Alfvénic turbulence was reached by Cohen and Dewar (1974) using a fluid model with the added assumption of strong damping of sound waves.

With the HELIOS-observations covering a rather broader frequency range than e.g. Coleman (1968) was able to use we may compare his turbulence model with the observations and in addition study the evolution of the turbulence from  $0.29\text{ AU}$  to  $1.0\text{ AU}$ . Besides differential flow HELIOS plasma observations show other sorts of internal particle energy in the high speed solar wind as beam-proton and alpha-particle relative streaming energy (Marsch et al., 1982a, b) being available as sources to drive the turbulence.

From the observed power spectra it appears that in the high speed solar wind certain frequencies always exist where the power spectral density estimates remain equally steep independent of heliocentric distance and magnetic field strength. Between  $4 \times 10^{-3}\text{ Hz}$  and  $2\text{ Hz}$  the spectral exponent is  $1.7$ , with little variation. The spectra obtained in the center of the high speed stream (Fig. 3) are a good example of the constancy of the slope in this frequency range indicating the possible existence of a universal turbulence law. From these observations we suggest that for a stationary state of the turbulence the inertial range spectrum would cover approximately the frequency range from  $4 \times 10^{-3}\text{ Hz}$  to slightly below the proton gyrofrequency:  $4 \times 10^{-3}\text{ Hz} < f < 10^{-1}\text{ Hz}$ . As demonstrated above, this inertial range turbulence is composed of a hierarchy of Alfvén waves with a small admixture (say 5%) of magnetoacoustic waves and/or convected static structures. Since the inertial range spectral exponent in the centers and trailing edges of high speed streams seems to be extremely constant (from 13 April to 17 April the spectral exponent determined by a least mean squares fit varies from  $1.71$  to  $1.79$ ) we may try a comparison with theoretically predicted values. Kraichnan's turbulence theory predicted a spectrum proportional to  $k^{-3/2}$  in the inertial range of wave numbers. The spectral exponent  $\alpha$  for  $P(f') \sim f'^{-\alpha}$  found by us is different though not very much but systematically. However, this is not surprising, as Kraichnan's (1965) theory applies to an incompressible medium, and therefore does not admit coupling of Alfvénic to compressive “eddies”. A spectral exponent of  $1.7$  to  $1.8$  is – fortuitously or not – near the Kolmogorov  $5/3$  slope of isotropic turbulence.

The range of dissipation by proton cyclotron damping extends upward in frequency from the proton gyrofrequency. By cascading through the spectrum the energy in these waves is dissipated by heating the protons leading to a temperature increase  $T_{\perp}$  perpendicular to the background magnetic field with a simultaneous

cooling of  $T_{\parallel}$  and a resulting  $T_{\perp} > T_{\parallel}$  (Busnardo-Neto et al., 1976; Arunasalam, 1976). Conversely the ion-cyclotron instability driven by  $T_{\perp} > T_{\parallel}$  causes  $T_{\perp}$  to decrease and  $T_{\parallel}$  to increase (Cuperman and Sternlieb, 1975; Davidson and Ogden, 1975; Gary and Feldman, 1978). The plasma experiment on board HELIOS has observed such an increase of  $T_{\perp}/T_{\parallel}$  by up to a factor of 2 in the centers and trailing edges of high speed streams (Marsch et al., 1982a), whereas  $T_{\perp}/T_{\parallel}$  was always smaller than 1 in the slow speed solar wind. The frequency dependence in the dissipation-range spectrum is of the order of  $f^{-3}$ .

Following Coleman's model of turbulent flow the power spectra observed by HELIOS are adjacent to the energy range of the turbulence and may cover parts of it. Then the steepening of the spectra from 0.29 AU to 1.0 AU for frequencies below  $4 \times 10^{-3}$  Hz may have to do with a different amount of energy fed into the system by differential flow at different heliocentric distances; i.e. less energy is available at larger distances from the sun. However there is no apparent instability mechanism working in a way to explain the observations; i.e. a local instability of Kelvin Helmholtz type would produce waves close to the cyclotron frequencies (e.g. Dobrowolny, 1977).

The steepening of the low frequency part of the spectra may find another explanation by applying a recent MHD-turbulence model of Dobrowolny et al. (1980a, b) who suggest that a turbulent description can easily account for the properties indicated by present observations and is therefore more appropriate than a description in terms of simple waves. To a good degree this MHD-turbulence would be characterized by the absence of nonlinear wave interactions and would necessarily be a mixture of modes with polarization of Alfvénic and slow magnetosonic types, in his nomenclature.

Dobrowolny et al. explain the apparent contradiction – the presence of an almost structureless power spectrum and the absence of nonlinear wave interactions – by the interpretation that the property of the absence of nonlinear wave interactions is not a particular one of the solar wind turbulence but is a general outcome of the relaxation of an initially excited MHD turbulence, provided that this initial excitation is asymmetric, i.e. favours one sense of propagation of the Alfvénic fluctuations. The spectral exponent should be the Kraichnan exponent. If this model applies to the interplanetary magnetic field fluctuations observed by HELIOS then there should be no energy transfer across the spectrum. From HELIOS-observations Denskat et al. (1981) have demonstrated the existence of only outwardly propagating Alfvénic fluctuations. From the turbulence model of Dobrowolny et al. this final one mode state would not be a stationary one (this would require the continuous presence of the source) but rather a static state. Consequently, the spectral behavior between 0.29 AU and 1.0 AU could only be explained by a linear damping process. Considering low frequencies  $< 4 \times 10^{-3}$  Hz this damping must be frequency dependent if the mechanism of a relaxation of initially excited turbulence would operate also in this frequency range. However, the relaxation process to a completely asymmetric state may not be finished for long wave

periods. Dobrowolny et al. (1980b) give the relevant non linear time  $T^{\pm}$  (which should be much shorter than a typical convection time)

$$T^{\pm} \sim T_w \left( \frac{\langle B \rangle}{|\delta B^{\mp}|} \right)^2 \quad (5)$$

where  $T_w$  is the wave period and the  $\pm$  sign stands for the two possible modes. At 0.29 AU  $\frac{\delta B}{\langle B \rangle}$  is between 0.3 and 0.6 (Denskat and Neubauer, 1982). For a wave frequency of  $10^{-4}$  Hz this relevant nonlinear time comes out to be  $\sim 10^5$  sec, which is almost twice the convection time at a solar wind speed of  $750 \text{ km s}^{-1}$  (e.g. in the center of the high speed stream in Fig. 3). This indicates that at long wavelengths the relaxation state of the turbulence might not be reached. Long period waves may still interact nonlinearly possibly transferring energy from higher to lower wavenumbers. Such a mechanism is possible by induced scattering by isotropic particles (Livshits and Tsytovich, 1970) causing transformation of wave energy along the spectrum in the direction of lower frequencies. On the other hand Denskat and Neubauer (1982) did not find significant differences in the statistical properties of MHD waves e.g. at  $10^{-4}$  Hz and at  $10^{-2}$  Hz.

## Summary

By using HELIOS-2 observations of the interplanetary vector magnetic field we have presented power spectral density estimates from  $2.4 \times 10^{-5}$  Hz up to 470 Hz. The data were obtained with a fluxgate magnetometer and a search coil magnetometer experiment both provided by the Technical University of Braunschweig.

A general feature of the power spectra observed is a rapid change in the slope and a displacement of the power spectral density estimates between 2 Hz and 4.7 Hz. The change in the slope may easily be explained by different wave modes possible well below and well above the proton gyrofrequency. The interpretation of the spectral displacement by the cyclotron damping of the Alfvénic component of the magnetic fluctuations and the approximate continuity of the magnetoacoustic component as the proton gyrofrequency is passed not only provides a satisfactory explanation but may in addition act as a proof for the generally accepted idea that the MHD fluctuations consist, in the major part, of Alfvén waves with a small admixture of magnetoacoustic waves and/or static structures. Similar arguments may be used for the interpretation in terms of hydromagnetic turbulence. Such an interpretation fits the observations as well and may be a better choice in describing hydromagnetic solar wind fluctuations. The power spectra from the HELIOS observations suggest that the inertial range of the turbulence covers the frequency range from  $\sim 4 \times 10^{-3}$  Hz to slightly below the local proton gyrofrequency:  $4 \times 10^{-3} \text{ Hz} < f < 10^{-1} \text{ Hz}$ . With increasing heliocentric radius the overall power level decreases on average as well as the magnetic field strength. In addition there are differences in the evolution of the spectra with changing heliographic distance at different frequencies. From  $4 \times 10^{-3}$  Hz up to 470 Hz the slope of the spectra remains relatively the same

between 0.29 AU and 1.0 AU. Below  $4 \times 10^{-3}$  Hz the spectra are steepening with increasing heliocentric distance. This behaviour may indicate damping at the higher frequencies, growth at the lower frequencies, or an energy transfer from the higher to the lower wave frequencies.

In addition spectra are presented at different locations of a solar wind high speed stream, where the different solar wind stream conditions change amplitudes and slope of the spectra.

## References

- Arunasalam, V.: Quasilinear theory of ion-cyclotron-resonance heating of plasmas and associated longitudinal heating. *Phys. Rev. Lett.* **37**, 746-749, 1976
- Barnes, A.: Hydromagnetic waves and turbulence in the solar wind. *Solar and solar wind plasma physics*, Vol. 1, E.N. Parker, C.F. Kennel, and L.J. Lanzerotti, eds.: pp. 249-319. North Holland Publ. Comp. 1979
- Bavassano, B., Dobrowolny, M., Mariani, F., Ness, N.F.: Radial evolution of power spectra of interplanetary Alfvénic turbulence. *J. Geophys. Res.* **87**, 3617-3622, 1982
- Behannon, K.W.: Observations of the interplanetary magnetic field between 0.46 and 1 AU by the Mariner 10 spacecraft. *NASA X-692-76-2*, 1976
- Behannon, K.W.: Heliocentric distance dependence of the interplanetary magnetic field. *Rev. Geophys. Space Phys.* **16**, 125-146, 1978
- Beinroth, H.J., Neubauer, F.M.: Properties of whistler-mode waves between 0.3 and 1.0 AU from Helios observations. *J. Geophys. Res.* **86**, 7755-7760, 1981
- Bendat, J.S., Piersol, A.G.: *Random data: Analysis and measurement procedures*. New York: Wiley-Interscience 1971
- Burlaga, L.F., Turner, J.B.: Microscale "Alfvén waves" in the solar wind at 1 AU. *J. Geophys. Res.* **81**, 73-77, 1976
- Busnardo-Neto, J., Dawson, J., Kaminura, T., Lin, A.T.: Ion-cyclotron resonance heating of plasmas and associated longitudinal cooling. *Phys. Rev. Lett.* **36**, 28-31, 1976
- Cohen, R.H., Dewar, R.L.: On the backscatter instability of solar wind Alfvén waves. *J. Geophys. Res.* **79**, 4174-4178, 1974
- Coleman, P.J. Jr.: Turbulence, viscosity, and dissipation in the solar wind plasma. *Astrophys. J.* **153**, 371-388, 1968
- Cuperman, S., Sternlieb, A.: The relaxation of strongly anisotropic magnetized plasmas by electromagnetic ion-cyclotron instability. *Plasma Phys.* **17**, 699-705, 1975
- Davidson, R.C., Ogden, J.M.: Electromagnetic ion-cyclotron instability driven by ion energy anisotropy in high-beta plasmas. *Phys. Fluids* **18**, 1045-1050, 1975
- Dehmel, G., Neubauer, F.M., Lukoschus, D., Wawretzko, J., Lammers, E.: Das Induktionsspulen-Magnetometer-Experiment (E4). *Raumfahrtforschung* **19**, 241-244, 1975
- Denskat, K.U.: Wellen im solaren Wind im Frequenzbereich des Helios-Induktionsspulenexperimentes E4 und deren Dopplerverschiebung. *Forschungsbericht W 75-18* des Bundesministeriums für Forschung und Technologie, 1975
- Denskat, K.U., Burlaga, L.F.: Multispacecraft observations of microscale fluctuations in the solar wind. *J. Geophys. Res.* **82**, 2693-2704, 1977
- Denskat, K.U., Neubauer, F.M., Schwenn, R.: Properties of Alfvénic fluctuations near the sun: Helios-1 and Helios-2. *Proc. of the 4th Solar Wind Conference*, Burghausen, F.R.G., Rep. No. MPAE-W-100-81-31, 392-397, 1981
- Denskat, K.U., Neubauer, F.M.: Statistical properties of low frequency magnetic field fluctuations in the solar wind from 0.29 to 1.0 AU during solar minimum conditions: Helios-1 and Helios-2. *J. Geophys. Res.* **87**, 2215-2223, 1982
- Dobrowolny, M.: Velocity shear instabilities in high-beta collisionless plasmas. II *Nuovo Cim.* **37**, 113-130, 1977
- Dobrowolny, M., Mangenay, A., Veltri, P.: Properties of magnetohydrodynamic turbulence in the solar wind. *Astron. Astrophys.* **83**, 26-32, 1980a
- Dobrowolny, M., Mangenay, A., Veltri, P.: Fully developed asymmetric hydromagnetic turbulence in the interplanetary space. *Phys. Rev. Lett.* **45**, 144-147, 1980b
- Gary, S.P., Feldman, W.C.: A second order theory for  $\mathbf{k} \parallel \mathbf{B}_0$  electromagnetic instabilities. *Phys. Fluids* **21**, 72-80, 1978
- Gurnett, D.A., Frank, L.A.: Ion acoustic waves in the solar wind. *J. Geophys. Res.* **83**, 58-74, 1978
- Hedgecock, P.C.: A correlation technique for magnetometer zero level determination. *Space Sci. Instrum.* **1**, 83-90, 1975a
- Hedgecock, P.C.: Measurements of the interplanetary magnetic field in relation to the modulation of cosmic rays. *Solar Phys.* **42**, 497-527, 1975b
- Jenkins, G.M., Watts, D.G.: *Spectral analysis and its application*. San Francisco, California: Holden-Day 1968
- Kraichnan R.H.: Inertial-range spectrum of hydromagnetic turbulence. *Phys. Fluids* **8**, 1385-1387, 1965
- Kurth, W.S., Gurnett, D.A., Scarf, F.L.: High-resolution spectrograms of ion acoustic waves in the solar wind. *J. Geophys. Res.* **84**, 3413, 1979a
- Kurth, W.S., Ashour-Abdalla, M., Frank, L.A., Kennel, C.F., Gurnett, D.A., Sentman, D.D., Burek, B.G.: A comparison of intense electrostatic waves near  $f_{UHR}$  with linear instability theory. *Geophys. Res. Lett.* **6**, 487-490, 1979b
- Livshits, M.A., Tsytovich, V.N.: The spectra of magnetohydrodynamic turbulence in collisionless plasma. *Nucl. Fus.* **10**, 241-250, 1970
- Marsch, E., Mühlhäuser, K.H., Schwenn, R., Rosenbauer, H., Philipp, W., Neubauer, F.M.: Solar wind protons: Three-dimensional velocity distributions and derived plasma parameters measured between 0.3 and 1 AU. *J. Geophys. Res.* **87**, 52-71, 1982a
- Marsch, E., Mühlhäuser, K.H., Rosenbauer, H., Schwenn, R., Neubauer, F.M.: Solar wind helium ions: Observations of the Helios probes between 0.3 and 1 AU. *J. Geophys. Res.* **87**, 35-51, 1982b
- Montgomery, D.C., Tidmann, D.A.: *Plasma kinetic theory*. New York: McGraw-Hill 1964
- Musmann, G., Neubauer, F.M., Maier, A., Lammers, E.: Das Förstersonden-Magnetfeldexperiment (E2). *Raumfahrtforschung* **19**, 232-237, 1975
- Neubauer, F.M., Beinroth, H.J., Barnstorf, H., Dehmel, G.: Initial results from the Helios 1 search coil magnetometer experiment. *J. Geophys. Res.* **42**, 599-614, 1977a
- Neubauer, F.M., Musmann, G., Dehmel, G.: Fast magnetic fluctuations in the solar wind: Helios 1. *J. Geophys. Res.* **82**, 3201-3212, 1977b
- Neubauer, F.M., Barnstorf, H., Beinroth, H.J., Denskat, K.U., Musmann, G., Ruprecht, H., Volkmer, P.: Routineverarbeitung und physikalische Interpretation der Meßdaten des Förstersondenmagnetometers (E2) und des Induktionsspulenmagnetometers (E4) der Raumsonden Helios 1 und Helios 2. *Forschungsbericht W 81-039* des Bundesministeriums für Forschung und Technologie, 1981
- Sari, J.W., Valley, G.C.: Interplanetary magnetic field power spectra: Mean field radial or perpendicular to radial. *J. Geophys. Res.* **81**, 5489-5499, 1976

Received December 13, 1982; Revised August 18, 1983

Accepted August 31, 1983